1   **The Aqueous Degradation of Bisphenol A and Steroid Estrogens by Ferrate**

2

3   *C. Li^1, X. Z. Li^{2*}, N. Graham^3 and N .Y. Gao^1*

4   ^{1}*Department of Environmental Engineering, Tongji University,*

5   *Shanghai, China*

6   ^{2}*Department of Civil and Structural Engineering, The Hong Kong Polytechnic University,*

7   *Hong Kong, China*

8   ^{3}*Department of Civil and Environmental Engineering, Imperial College London, South Kensington*
9   *Campus, London SW7 2AZ, UK*

10

11   **Abstract**

12   The aqueous reactivity of five prominent endocrine disrupting chemicals (EDCs) with potassium

13   ferrate has been studied. The degradation kinetics and reaction pathways for bisphenol A (BPA)

14   have been considered in detail, and the reaction rate constants for 17α-ethynylestradiol (EE2),

15   estrone (E1), *β*-estradiol (E2), and estriol (E3) have been determined, from tests carried out in the

16   pH range of 8-12 and at different reactant molar ratios. The rate constants were determined by a

17   kinetic model incorporating the various species equilibria for the EDC compounds and ferrate,

18   using observations of the temporal reduction in EDC and ferrate concentrations. In agreement with

19   other studies the oxidation of the EDCs was found to be greater for mono-protonated

20   ferrate, $HFeO_4^-$, than for non-protonated ferrate, FeO_4^{2-}. Among the five EDCs, which all have

21   phenol moieties, the ferrate oxidation of the four steroid estrogens (each incorporating the

22   cyclopentanoperhydrophenanthrene ring) had higher reaction rates than BPA. The by-products of

23   BPA degradation by ferrate were analyzed by LC/MS-MS and GC/MS-MS and nine specific

24   compounds   were   identified,   including   *p*-isopropylphenol,   *4*-isopropanolphenol,

25   *p*-isopropenylphenol, and some dicarboxylic acids etc. It is concluded that ferrate oxidation could

26   be an effective treatment method for the purification of waters containing these particular EDCs.

27

28   ***Keywords:*** Bisphenol A; BPA; Endocrine disruptor; Fe(VI); Potassium ferrate; Steroid estrogens**.**

---

* *Corresponding author: phone: (852) 2766 6016; Fax: (852) 2334 6389; Email: cexzli@polyu.edu.hk (X. Z. Li)*

1. Introduction

A number of chemicals exist in the environment that affect the endocrine system and produce an adverse effect on aquatic life, animals and potentially humans (Fry, 1995; Sumpter, 1995). There is increasing evidence that these compounds can alter endocrine functions and may disrupt growth, development, and reproduction by interfering with the production of the endocrine system. Accordingly, because of the role of estrogenic chemicals, often referred to as environmental estrogens, in contributing to the development of hormone-dependent cancers, disorders of the reproductive tract, and other effects (Folmar et al., 1996; Toppari et al., 1996), they are classified as "endocrine disrupting chemicals" (EDCs). EDCs have generated a vast amount of attention among the scientific, research and regulatory communities worldwide (Birkett and Lester, 2003).

Among prominent EDCs of interest currently, this study has considered two synthetic endocrine disrupting chemicals, bisphenol A (BPA) and 17α-ethynylestradiol (EE2), and three natural EDCs, estrone (E1), 17β-estradiol (E2), and estriol (E3), which have been chosen for their environmental significance. BPA, also known as 2,2-bis-(4-hydroxy-phenyl) propane or 4,4'-isopropylidenediphenol, is an important monomer chemical used for the production of various polycarbonate and polysulphone plastics and epoxy resins. It is a known EDC due to its estrogenicity, with about 500 times the estrogenic activity of octylphenol (Nagel et al., 1997). In addition, it has been reported to cause reproductive toxicity and to affect cellular development in rats and mice and is generally regarded as a serious contributor to water pollution (Real et al., 1985; Morrisey et al., 1987; Williams et al., 1996; Sajiki et al., 2001).

The steroid compounds, E1, E2, E3 and EE2, are derived from the biotransformation of cholesterol, a precursor of mammalian sexual steroids (Williams et al., 1996). The female body naturally produces the three estrogens, E1, E2 and E3, but they are also present in males, although

generally at much lower levels (Snyder et al., 1999). The synthetic estrogen EE2 (17α-ethynyl-1,3,5(10)-estratriene-3,17β-diol) is not only a key ingredient in oral contraceptives used by western women since the 1960s, but is also a hormonal agent used in the stockbreeding industry. All four steroid compounds have been reported to be responsible for a large part of the estrogenicity burden of municipal wastewaters (Ning et al., 2007), and E2 and EE2 have been shown to elicit a range of physiological effects in organisms at very low concentrations (Christiansen et al., 2006). In general, the steroid compounds and BPA are considered to be incompletely removed by conventional secondary wastewater treatment processes; for example, Ternes et al. (Ternes et al., 1999) confirmed that an activated sludge in batch experiment systems removed only 20% of the initial amount of EE2 (1 μg L^{-1}) in 24 h to 48 h, and the concentration of the remaining EE2 did not decrease further. Thus, these chemicals, which are described in Table 1, were chosen for our study because of their environmental importance and because they have a common phenolic moiety.

[Table 1]

In view of their presence in conventionally treated effluents, and the need to mitigate their discharge into natural water bodies, the comparative performance of additional, alternative treatment technologies is of considerable interest to water utilities and regulatory authorities at the moment. Among the treatment methods being evaluated currently are oxidation by ozone (Ning et al., 2007) and chlorine dioxide, and adsorption by activated carbon. Another strong oxidant, potassium ferrate, is receiving considerable attention at present owing to the high redox potential of the ferrate(VI) ion from 2.2 V to 0.7 V in respectively, acidic and basic solutions (Sharma, 2002), and associated coagulation effect arising from the reduced Fe(III) species for metals, nonmetals, and radionuclides from solution (Jiang and Lloyd, 2002; Sharma et al., 2005). Ferrate(VI) has

1   powerful disinfection properties that enables it to inactivate a wide variety of microorganisms at

2   low Ferrate(VI) dosages including many chlorine resistant organisms (Sharma, 2007; Jiang et al.,

3   2006). Moreover, unlike ozone, Ferrate(VI) does not react with bromide ions, thus avoiding the

4   possible formation of the suspected carcinogenic bromate ion in the treatment of

5   bromide-containing water by ferrate(VI) (Sharma et al., 2006).

6   The objective of this study was to evaluate the ferrate(VI) oxidation of the five previously

7   mentioned EDCs, with particular emphasis on the reaction pathways of BPA. The evaluation of

8   BPA follows an earlier preliminary investigation carried out by the authors (Li et al., 2005). The

9   reaction rate constants were determined by a kinetic model incorporating the various species

10   equilibria for the EDC compounds and ferrate, using observations of the temporal reduction in EDC

11   and ferrate concentrations. In addition to reporting on the rate constants, we have investigated the

12   completeness of the BPA degradation and have identified some of the intermediate products by

13   liquid chromatography/mass spectrometry-mass spectrometry (LC/MS-MS) and gas

14   chromatography/mass spectrometry-mass spectrometry (GC/MS-MS).

15

16 **2. Materials and methods**

17 *2.1. Chemicals*

18   The Fe(VI) chemical was prepared in the laboratory as potassium ferrate (K_2FeO_4) with high

19   purity (99%) by a previously optimized method based on the oxidation of ferric nitrate with

20   hypochlorite (Li et al., 2005). The principal chemicals employed in the laboratory experiments were

21   purchased as analytical grade, and used without further purification. These included $Fe(NO_3)_3.9H_2O$

22   (>98%) from Acros, potassium hydroxide from BDH, potassium permanganate from Sigma Aldrich,

23   dichloromethane from Redel-deHaën; the EDCs (BPA, E1, E2, E3, and EE2) were all obtained from

Sigma Aldrich. The solutions were prepared with water that had been distilled and then passed through an 18MΩ Milli-Q water purification system.

2.2. Analytical Equipment and Methods

2.2.1 HPLC

The concentrations of the five EDCs were determined using high performance liquid chromatograph (HPLC) incorporating a high pressure pump (Spectrasystem HPLC P4000), a UV detector (UV 6000LP), and an auto sampler (AS3000). In the HPLC analysis, a pinnacle II C18 column (5 μm particle size, 250 mm length, and 4.6 mm inner diameter) and a mobile phase of acetonitrile/water (7:3, v/v) at a flow rate of 0.8 ml min^{-1} were used. The method involved an injection volume of 20 μl and UV detection of the five EDCs in the range of 278-281 nm; the specific retention times and detection wavelengths of the compounds are shown in Table 2.

[Table 2]

2.2.2. LC/MS-MS and DOC

Liquid chromatography together with electrospray-ionization mass spectrometry (LC-ESI-MS), Finnigan ThermoQuest LCQ Duo, was used to detect the intermediate products of BPA degradation. In this study, the mass spectrometer was operated in the m/z 100-300 range for LC/MS-MS. The eluent was delivered at 0.7 ml min^{-1} by a gradient system from HPLC and partitioned by a pinnacle II C18 column. The elution was carried out with a gradient flow as described in Table 3:

[Table 3]

The LC eluent was directed to the ESI detector for the detection of negative ions [M-H]$^-$ and positive ions [M+H]$^+$. The ESI probe was installed with sheath and auxiliary gases running at 60

and 20 unites respectively. The MS conditions were as follows: the capillary temperature was set at 250 $^{\circ}$C with a voltage of 46 V and a spray voltage of 4.5 kV. In this study, dissolved organic carbon (DOC) of samples was determined by a total organic carbon (TOC) analyzer (Shimadzu TOC-5000A).

2.2.3. GC/MS-MS

Gas chromatography-mass spectrometry (GC/MS-MS) analyses were performed by Varian 3800GC and Varian 1200Mass, equipped with a fused silica capillary column (Varian VF-5 ms, 30 m long, 0.25 mm i.d., 0.25 μm D.F.). The column temperature was programmed as follows: 1 min at 50 °C, 10 °C min^{-1} to 150 °C, and then 30 °C min^{-1} to 280 °C. Electron impact was used for the ionization of samples for the GC/MS-MS analysis. The identification of the intermediates was made by using an identification program from the US National Institute of Standards and Technology (NIST) library. The intermediate products of BPA during ferrate(VI) oxidation were extracted by dichloromethane. The samples were taken at different time intervals and put into concentrated HCl to produce a pH < 2 solution. The resulting solutions were saturated with 2.5 g sodium chloride and then underwent compound extraction with dichloromethane (3 × 2 mL). The combined dichloromethane extracts were dried with anhydrous sodium sulfate.

In order to identify low-molecular-weight (LMW) intermediate products from BPA degradation by potassium ferrate, the butyl-esterification derivatization method was applied. The method based on the previous work by Li and Yu in 2005 was developed to measure the intermediate products of BPA degradation more easily for a larger range of compounds; this is described as follows.

Samples taken at different time intervals were evaporated under a vacuum. Concentrated HCl

was introduced to the samples to produce a pH < 2 solution. The resulting solution was saturated

with 2.5 g sodium chloride, and then solutions were extracted with diethyl ether (3 × 10 mL). The

combined ether extracts were dried with anhydrous sodium sulfate and the ether was evaporated

under N_2. The residue was dissolved in 2 mL of methanol and then 0.3 mL of BF_3/MeOH added to

the residue. The solution was heated to about 90-100 ^{o}C for 30 min, and after cooling the residue

was extracted with a mixture of 2 ml n-hexane, 2 ml water, and 0.2 ml acetonitrile; the acetonitrile

allows more effective transfer of methanol into the aqueous phase. The extraction step was repeated

twice and the resulting extracts were combined. The hexane layer was reduced to about 200 μL by

evaporation under N_2, and trace amounts of water were removed by anhydrous Na_2SO_4. A quantity

of 50 μl tetracosane–D_{50} was added to the residue solution and the resulting derivatives were

injected into the GC-MS system (Agilent 6890 GC and 5793 MS) for analysis.

2.2.4. Degradation of EDCs

Aqueous EDC compounds ([BPA]$_0$ = 0.1 mM, [EE2]$_0$ = 0.01 mM, [E1]$_0$ = 0.01 mM, [E2] = 0.01

mM, [E3] = 0.01 mM) and potassium ferrate solutions ([Fe(VI)]$_0$ = 0.05-0.5 mM) were prepared

with deionized distilled water and pH buffer solution, and the Fe(VI) solution was freshly prepared

just prior to each test owing to its rapid decomposition in aqueous solution. The oxidation tests were

carried out in the pH range of 8.2-12, and with different molar ratios of the reactants. In each

oxidation test, samples were taken at distinct time intervals up to 10 min. Sodium sulfite solution

(10 M) was added immediately to each sample upon removal from the reaction in order to quench

the ferrate and stop any further oxidation. All the oxidation tests were carried out at room

temperature (about 25 ^{o}C).

3. Results and Discussion

3.1. Kinetics of EDCs degradation by ferrate(VI) oxidation

To study the degradation kinetics of the EDCs by ferrate(VI) oxidation, several sets of tests were carried out at different pH values from pH 8.2 to pH 12, with the following initial reactant concentrations: $[BPA]_0 = 0.1$ mM, $[EE2]_0 = 0.01$ mM, $[E1]_0 = 0.01$ mM, $[E2] = 0.01$ mM, $[E3] = 0.01$ mM, and $[Fe(VI)]_0 = 0.05\text{-}0.5$ mM. A kinetic model based on a second-order reaction was developed by considering that both the ferrate and the EDCs are dissociating compounds in aqueous conditions. For the pH conditions used in this study the ferrate is assumed to be in either the mono-protonated ($HFeO_4^-$, pKa = 7.23), or dissociated (FeO_4^{2-}) form, and the EDC is either non-dissociated (EDC') or dissociated (EDC^-); the pKa values for the EDCs are given in Table 1. The oxidation reactions are summarized as follows:

$$(\frac{d[EDC]}{dt})_1 = -[FeO_4^{2-}](k_1[EDC^{'}] + k_1^{'}[EDC^-]) \tag{1}$$

$$(\frac{d[EDC]}{dt})_2 = -[HFeO_4^-](k_2[EDC^{'}] + k_2^{'}[EDC^-]) \tag{2}$$

The overall rate of EDC compound degradation is assumed to be the sum of these two rates and can be expressed by Eq. (3).

$$\frac{d[EDC]}{dt} = (\frac{d[EDC]}{dt})_1 + (\frac{d[EDC]}{dt})_2 \tag{3}$$

The corresponding rates of oxidant (FeO_4^{2-} and $HFeO_4^-$) reduction during the reaction can be expressed by Eqs. (4) and (5), respectively:

$$\frac{d[FeO_4^{2-}]}{dt} = -[FeO_4^{2-}](k_{11}[EDC^{'}] + k_{11}^{'}[EDC^-]) \tag{4}$$

$$\frac{d[HFeO_4^-]}{dt} = -[HFeO_4^-](k_{21}[EDC^{'}] + k_{21}^{'}[EDC^-]) \tag{5}$$

In the case of the ferrate reduction, the overall rate of ferrate(VI) reduction can be assumed to be the sum of the two rates, plus the thermodynamic decomposition of ferrate in water; this can be expressed by Eq. (6).

1     $\dfrac{d[Fe(VI)]}{dt} = \dfrac{d[FeO_4^{2-}]}{dt} + \dfrac{d[HFeO_4^{-}]}{dt} - k_d[Fe(VI)]$ (6)

2   where k_d is the decomposition constant of ferrate(VI) in the solution.

3   Our previous work (Li et al., 2005) confirmed that the aqueous decomposition of potassium

4   ferrate at pH 8.5 to 9.5 is very slow (< 5% after 20 min at room temperature). Therefore, in this pH

5   range the overall rate expression can be simplified as:

6     $\dfrac{d[Fe(VI)]}{dt} = \dfrac{d[FeO_4^{2-}]}{dt} + \dfrac{d[HFeO_4^{-}]}{dt}$ (7)

7   According to the equilibrium of the two ferrate species at different pH, the concentrations of

8     $HFeO_4^{-}$ and FeO_4^{2-} should have a specific ratio at a given pH, as shown below:

9     $[HFeO_4^{-}] = \alpha_{HFeO_4^{-}}[Fe(VI)] = \dfrac{[HFeO_4^{-}]}{[Fe(VI)]}[Fe(VI)]$ (8)

10    $[FeO_4^{2-}] = \alpha_{FeO_4^{2-}}[Fe(VI)] = \dfrac{[FeO_4^{2-}]}{[Fe(VI)]}[Fe(VI)]$ (9)

11

12   Moreover, the relationship between the concentrations of undissociated and dissociated EDCs and

13   pH can be described by the following expressions:

14    $[EDC^{-}] = \dfrac{k_{aEDC}}{[H^{+}] + k_{aEDC}}[EDC]$ (10)

15    $[EDC'] = \dfrac{[H^{+}]}{[H^{+}] + k_{aEDC}}[EDC]$ (11)

16   Therefore, Eqs. (3) and (7) can be expressed by Eqs. (12) and (13).

17    $\dfrac{d[EDC]}{dt} = -(k_1\alpha_{FeO_4^{2-}} \times \dfrac{[H^{+}]}{[H^{+}]+k_{aEDC}} + k_1'\alpha_{FeO_4^{2-}} \times \dfrac{k_{aEDC}}{[H^{+}]+k_{aEDC}} + k_2\alpha_{HFeO_4} \times \dfrac{[H^{+}]}{[H^{+}]+k_{aEDC}} + k_2'\alpha_{HFeO_4} \times \dfrac{k_{aEDC}}{[H^{+}]+k_{aEDC}})[EDC][Fe(VI)]$

18    $= k_e[EDC][Fe(VI)]$ (12)

19

20    $\dfrac{d[Fe(VI)]}{dt} = -(k_{11}\alpha_{FeO_4^{2-}} \dfrac{[H^{+}]}{[H^{+}]+k_{aEDC}} + k_{11}'\alpha_{FeO_4^{2-}} \dfrac{k_{aEDC}}{[H^{+}]+k_{aEDC}} + k_{21}\alpha_{HFeO_4} \dfrac{[H^{+}]}{[H^{+}]+k_{aEDC}} + k_{21}'\alpha_{HFeO_4} \dfrac{k_{aEDC}}{[H^{+}]+k_{aEDC}}[EDC][Fe(VI)]$

21    $= k_f[EDC][Fe(VI)]$ (13)

22   Dividing Eq. (12) by Eq. (13) and intergrating $d[EDC] = \dfrac{k_e}{k_f}d[Fe(VI)]$ with the initial conditions

(when t = 0, [EDC] = [EDC]$_0$ and [Fe(VI)] = [Fe(VI)]$_0$), a pair of second-order equations for EDC degradation and Fe(VI) reduction versus reaction time are expressed by Eqs. (14) and (15), respectively.

$$[EDC] = \frac{k_e[EDC]_0[Fe(VI)]_0 - k_f[EDC]_0^2}{k_e[Fe(VI)]_0 e^{(k_e[Fe(VI)]_0 - k_f[EDC]_0)t} - k_f[EDC]_0} \tag{14}$$

$$[Fe(VI)] = \frac{k_f[EDC]_0[Fe(VI)]_0 - k_e[Fe(VI)]_0^2}{k_f[EDC]_0 e^{(k_f[EDC]_0 - k_e[Fe(VI)])t} - k_e[Fe(VI)]_0} \tag{15}$$

where $k_e = \dfrac{k_1 k_{aFE}[H^+] + k_1' k_{aFE} k_{aEDC} + k_2[H^+]^2 + k_2'[H^+]k_{aEDC}}{[H^+]^2 + [H^+]k_{aEDC} + [H^+]k_{aFE} + k_{aFE}k_{aEDC}}$

$k_f = \dfrac{k_{11} k_{aFE}[H^+] + k_{11}' k_{aFE} k_{aEDC} + k_{21}[H^+]^2 + k_{21}'[H^+]k_{aEDC}}{[H^+]^2 + [H^+]k_{aEDC} + [H^+]k_{aFE} + k_{aFE}k_{aEDC}}$

The rate constants, k_1, k_1', k_2, k_2', k_{11}, k_{11}', k_{21}, and k_{21}' were determined by the least square method via the Matlab 6.5 program (MathWorks, Inc.), and the values for the EDC degradation rate (k_1, k_1', k_2, and k_2') are listed in Table 4. The fitted results and experimental observations at pH 9.2 with [EE2]$_0$ = 0.01 mM, [E1]$_0$ = 0.01 mM, [E2]$_0$ = 0.01 mM, [E3]$_0$ = 0.01 mM, [BPA]$_0$ = 0.1 mM and [Fe(VI)]$_0$ = 0.05 or 0.1 mM, are shown in Fig. 1.

[Fig. 1]

[Table 4]

It can be seen from Fig. 1 that the second-order reaction model fitted the experimental degradation data closely (R^2 = 0.992-0.998). Thus, the results indicated that the modelling can adequately describe both the kinetics of BPA degradation and ferrate reduction in aqueous solution. Moreover, the rate constants shown in Table 4 indicate that the oxidizing power of mono-protonated ferrate, $HFeO_4^-$, is greater than non-protonated ferrate, FeO_4^{2-}, for all of the EDCs, and that the dissociated (ionized) EDCs are more reactive, particularly with mono-protonated ferrate (by 2-2½

1 orders of magnitude), than with undissociated EDCs. In a previous study (Lee et al., 2005) it was

2 assumed that the reactions of H_2FeO_4 and FeO_4^{2-} with the phenolic EDCs did not contribute

3 significantly to the overall reaction and thus were neglected in the model calculations. Moreover,

4 the following reactions were considered and the reaction rates are shown in Table 4:

5 $HFeO_4^- + EDC(EE2, E2, or\ \ BPA) \xrightarrow{\ k_{21}\ } products$

6 $HFeO_4^- + EDC^-(EE2^-,\ \ E2^-,\ \ or\ \ BPA) \xrightarrow{\ k_{22}\ } products$

7 $HFeO_4^- + EDC^{2-}(BPA^{2-}) \xrightarrow{\ k_{23}\ } products$
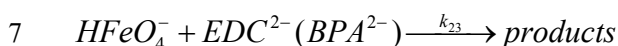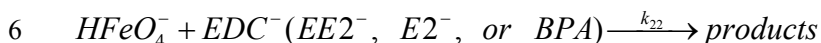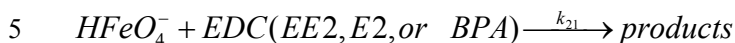
8 As FeO_4^{2-} is the main form of Fe(VI) at pH > 8, the rate constants for FeO_4^{2-} and phenolic EDCs

9 need to be considered at high pH. By comparing the rate constants determined here with those of

10 Lee et al. (2005), we find similar values for $HFeO_4^-$ with undissociated and dissociated forms of

11 BPA, EE2 and E2. At the same time, we observe that the rate constant values of FeO_4^{2-} and

12 dissociated forms of EDCs are similar with the rate constant values of $HFeO_4^-$ and undissociated

13 forms of EDCs. Therefore, the reactions of FeO_4^{2-} and dissociated forms of EDCs need to be

14 considered in the model calculations. In order to compare the rate constants of Fe(VI) and phenolic

15 EDCs, this paper has considered only two species of BPA and found similar rate constants between

16 Fe(VI) and phenolic EDCs.

17

18 *3.2. Pathways of BPA degradation with ferrate(VI)*

19   The identification of reactions products from the oxidation of BPA by ferrate was attempted by

20 means of the LC/MS-MS, GC/MS-MS and TOC analytical methods. In the HPLC analysis with

21 flow injection of BPA standard solutions, the m/z 227 ion, assigned the [M-H]⁻ ion, was observed as

22 the principal peak, as shown in Fig. 2.

23   **[Fig. 2]**

1 This is explained by the characteristic cleavage of the O-H bond in the hydroxyl group and a

2 fragment ion at m/z 212, resulting from a cleavage of one of the -CH_3 groups is observed. The

3 degree of mineralization of BPA with ferrate oxidation was investigated by analyzing the variation

4 of the DOC concentration during the reaction. The results about the variation of soluble organic

5 carbon concentration during BPA degradation with ferrate(VI) at pH 9.2 with an initial BPA

6 concentration of 23 mg L^{-1} (or 18 mg L^{-1} carbon) are shown in Fig. 3.

7 **[Fig. 3]**

8 It is seen from Fig. 3 that the soluble organic carbon content decreased continuously with

9 reaction time, which indicates partial mineralization of the parent compound and reaction products

10 in the system to carbon dioxide. With increasing ferrate(VI) dose (ferrate:BPA ratio) and the DOC

11 decreasing from 60% to 20%, it was also evident that the extent of mineralization increased

12 systematically. The difference between the degrees of degradation and mineralization for

13 ferrate:BPA ratios greater than 1, indicates that some intermediate products of BPA degradation

14 remained at 10 min under these experimental conditions; for the case of ferrate:BPA ratio of 4:1 and

15 5:1, the BPA had disappeared completely by 8 minutes while significant DOC was present. The

16 continuous reduction in DOC with reaction time showed that less accumulation in the total

17 concentration of intermediates was achieved at a higher ferrate:BPA ratio and some intermediated

18 are mineralized by the excess ferrate.

19 In this study, the intermediate compounds from the BPA-ferrate reaction with relatively large

20 molecular weight (molecule weight >100) were analyzed by LC/MS-MS, since the ion trap mass

21 spectrometer (Finnigan Duo LCQ-ms/ms) is only suitable for analyses corresponding to m/z $\geq$100.

22 In the negative ion mode, the product ion spectra revealed the main fragments (m/z) and

23 abundances [%] obtained for peaks 1-4, as summarized in Table 5. The m/z values for each peak

1   corresponds to [M-1]⁻ ions in the negative ion mode of LC/MS-MS. For example, the m/z value of

2   BPA should be 228 but was detected as 227, which is explained by the characteristic cleavage of the

3   O-H bond in the hydroxyl group. It is seen from Table 5 that the three peaks had retention times less

4   than BPA which indicates that they are more polar than BPA. Fig. 4 shows the formation and decay

5   of the three identified intermediate products (peaks 1-3) formed during the ferrate and BPA reaction.

6   **[Fig. 4]**

7   Four peaks (1-4) appeared in the HPLC chromatogram and the vertical axis in Fig. 4 corresponds

8   to the heights of the absorption peaks normalized to the height of the initial BPA peak. The

9   maximum absorbance values for the three products were reached after approximately 4 min (peaks

10 3, 2, and 1). However, all of the peaks had almost disappeared after 20 min of ferrate oxidation.

11 From the LC/MS-MS analyses described above the intermediate compounds were identified as

12 *4*-isopropanolphenol, *p*-isopropylphenol, and *p*-isopropenylphenol. Peak 1 of the LC/MS-MS

13 spectrum exhibits a parent peak at m/z 134, which was identified as *p*-isopropenylphenol. Peak 2

14 exhibits a parent peak at m/z 136, with fragment ion peaks at [M-1-15] = 120 and [M-1-42] = 93,

15 indicating the loss of $-CH_3$ and $-CH_3CCH_3$ groups respectively. The remaining values can be

16 explained by the loss of a phenyl group of BPA to give $[M_{BPA}-92]$ = 136. The parent peak of peak 2

17 was identified as *p*-isopropylphenol (IPP). Peak 3 of the LC/MS-MS spectrum exhibits a parent

18 peak at m/z 152, which was identified as *4*-isopropanolphenol.

19 The identity of other intermediate products from BPA degradation was also evaluated by

20 GC/MS-MS which is particularly suitable for the relatively smaller molecular weight compounds.

21 Several compounds were evident from the GC/MS-MS chromatogram as summarised in Table 6.

22 **[Table 6]**

23 In addition, a butyl-esterification derivative method was used to enhance the effectiveness of the

1 GC/MS-MS method. From this, some low-molecular-weight intermediate products were identified,

2 as shown in Table 7.

3 **[Table 7]**

4 Table 7 summarizes the main fragments (m/z) obtained for the intermediate products during the

5 reaction time of 20 min as detected by the GC/MS-MS method and comparing the mass spectra

6 with the NIST data library. The variation in the amounts of intermediate products formed during the

7 BPA degradation is shown in Fig. 5.

8 **[Fig. 5]**

9 It is seen from Fig. 5 that the maximum values of the identified intermediate products were reached

10 at approximately 6 min of reaction time, and decreased substantially with increased reaction time up

11 to 20 min.

12 From the GC/MS-MS analysis, the intermediate compounds that were identified were oxalic acid,

13 propanedioic acid, *4*-isopropyl-cyclohexa-2,5-dienone, *p*-hyroxyacetophenone, *p*-isopropenylphenol,

14 styrene and (1-phenyl-1-butenyl)benzene. Overall, nine intermediate compounds were found from

15 the combined LC/MS-MS and GC/MS-MS analyses, with *p*-isopropenylphenol identified by both

16 analyses. Based on these identified intermediate products, the pathways for the BPA degradation by

17 ferrate are proposed schematically in Fig. 6.

18 **[Fig. 6]**

19 During the initial oxidation reaction, the bond of the two phenyl groups in BPA is cleaved

20 because the electron-donating hydroxyl group increases the electron density of each aromatic ring,

21 and the bond connecting with two aromatic rings becomes more vulnerable. Therefore, BPA can be

22 degraded to *p*-isopropylphenol, phenol, *4*-isopropanolphenol, and (1-phenyl-1-butenyl)benzene.

23 These intermediate products can in turn be degraded by ferrate, producing styrene,

14

p-hydroxyacetophenone, *4*-isopropyl-cyclohexa-2,5-dienone, propanedioic acid and oxalic acid. Ohko et al. (Ohko et al., 2001) also reported the formation of these products during BPA photodegradation by TiO_2 photocatalysis, but the (1-phenyl-1-butenyl) benzene and styrene were not detected during the photocatalysis. This suggests that there may be some differences in the degradation pathway for BPA when reacting with ferrate compared to photocatalytic degradation.

Conclusions

In this paper the reaction rate constants for bisphenol A (BPA), 17α-ethynylestradiol (EE2), estrone (E1), *β*-estradiol (E2), and estriol (E3) have been determined, from tests carried out in the pH range of 8-12 at different reactant molar ratios. The rate constants were determined by a second-order kinetic model incorporating the various species equilibria for the EDC compounds and ferrate, using observations of the temporal reduction in EDC and ferrate concentrations. In general, the application of potassium ferrate can achieve a major removal of these compounds. The extent of the treatment will vary with the aqueous conditions since pH, in particular, affects the nature of the ferrate ion and the degree of EDC dissociation. In agreement with other studies, the oxidation of the EDCs was found to be greater for mono-protonated ferrate, $HFeO_4^-$, than for non-protonated ferrate, FeO_4^{2-}. Among the five EDCs, the ferrate oxidation of the four steroid estrogens was greater (higher reaction rates) than that of BPA.

The reaction of BPA with ferrate was studied in detail in order to identify the formation of intermediate reaction products and clarify the BPA degradation pathway. From the analyses by LC/MS-MS and GC/MS-MS, nine specific compounds were identified, including *p*-isopropylphenol, *p*-isopropenylphenol, *4*-isopropanolphenol, and dicarboxylic acids (eg. oxalic acid). Whilst under some conditions (e.g. ferrate:BPA molar ratio ~ 5:1) BPA can be completely

degraded in less than 5 minutes, the degree of organic mineralization was significantly less than 100%, indicating the presence of reaction products which persist well beyond the disappearance of the BPA.

Overall, given that the molar ratio of ferrate to EDCs in practice would be several orders of magnitude, it is concluded that ferrate oxidation could be an effective treatment method for the purification of waters containing these particular EDCs.

Acknowledgements

References

Birkett, J.A., Lester, J.N., editors, 2003. Endocrine disruptors in wastewater and sludge treatment processes. Boca Raton, Florida: CRC Press LLC, p. 119-125.

Christiansen, L.B., Winther-Nielsen, M., Helwig, C., July 2006. The effect of estrogenic compounds and their fate in sewage treatment plants and nature. http://www.mst.dk/udgiv/publications/2002/87-7972-305-5/html/default_eng.htm.

Folmar, L.C., Denslow, N.D., Rao, V.M., Chow, D.A., Crain, Enblom, J., Marcino, J., Guillette, J.R.L.J., 1996. Vitellogenin induction and reduced serum testosterone concentrations in feral male carp (Cyprinus carpio) captured near a major metropolitan sewage treatment plant. Environ. Health. Persp. 104, 1096-1101.

1   Fry, D.M., 1995. Reproductive effects in birds exposed to pesticides and industrial chemicals.

2   Environ. Health. Persp. 311, 65-171.

3   Jiang, J.Q., Lloyd, B., 2002. Progress in the development and use of ferrate(VI) salt as an oxidant

4   and coagulant for water and wastewater treatment. Water Res. 36, 1397-1408.

5   Jiang, J.Q., Wang S., Panagoulopoulos A., 2006. The exploration of potassium ferrate(VI) as a

6   disinfectant/coagulant in water and wastewater treatment. Chemosphere 63, 212-219.

7   Kawamura, K., Steinberg, S., Kaplan, I.R., 1985. Capillary GC determination of short-chain

8   dicarboxylic acids in rain, fog, and mist. Int. J. Environ. Anal. Chem. 19, 175-188.

9   Kawamura, K., 1993. Identification of C2-C10 *ö*-oxocarboxylic acids, pyruvic acid, and C2-C3

10   R-dicarbonyls in wet precipitation and aerosol sample by capillary GC and GC/MS. Anal.

11   Chem. 65, 3505-3511.

12   Lee, Y.H., Yoon, J.Y., von Gunten, U., 2005. Kinetics of the oxidation of phenols and phenolic

13   endocrine disruptors during water treatment with ferrate (Fe(VI)). Environ. Sci. Technol. 39,

14   8978-8984.

15   Li, C., Li, X.Z., Graham, N., 2005. A study of the preparation and reactivity of potassium ferrate.

16   Chemosphere 61, 537-543.

17   Li, Y.C., Yu, J.Z., 2005. Simultaneous determination of mono- and dicarboxylic acids,

18   w-oxo-carboxylic acids, midchain ketocarboxylic acids, and aldehydes in atmospheric aerosol

19   samples. Envion. Sci. Technol. 39, 7616-7624.

20   Morrisey, R.E., George, H.D., Price, C.J., Tyl, R.W., Marr, M.C., Kimmel, C.A, 1987. The

21   developmental toxicity of bisphenol-A in rates and mice. Fundam. Appl. Toxical. 8, 571-582.

22   Nagel, S.C., VomSaal, F.S., Thayer, K.A., Dhar, M.G, Boechler, M., Welshons, W.V., 1997.

23   Relative binding affinity serum modified access (RBA-SMA) assay predicts the relative in

vivo bioactivity of the xenoestrogens bisphenol A and octylphenol. Environ. Health Persp. 105, 70-76.

Ning, B., Graham, N., Zhang, Y., Nakonechny, M. and Gamal El-din, M. (2007). 'Degradation of Endocrine Disrupting Chemicals by Ozone and AOPs'. Ozone: Sci and Eng, 29, 153-176.

Ohko, Y., Ando, I., Niwa, C., Tatsuma, T., Nakashima, T., Kubota, Y., Fujishima, A., 2001. Degradation of Bisphenol A in water by TiO_2 photocatalyst. Environ. Sci. Technol. 35, 2365-2368.

Real, J.R., George, J.D., Lawton, A.D., Myers, C.B., Lamb, J.C., 1985. Bisphenol A: Reproduction and fertility assessment in CD-1 mice when administered in feed:NTP/NIEHS Report. Research Triangle Park, NC.

Sajiki, J., 2001. Determination of bisphenol-A in blood using high-performance liquid chromatography-electrochemical detector with solid-phase extraction. J. Chromatogr. B 955, 9-15.

Sharma, V.K., 2002. Potassium ferrate(VI): an environmentally oxidant. Adv. Environ. Res. 6, 143-156.

Sharma, V.K., Burnett C.R., Yngard R.A., Cabelli D.E., 2005. Iron(VI) and Iron(V) oxidation of copper(I) cyanide. Environ. Sci. Technol. 39, 3849-3854.

Sharma, V.K., Mishra, S.K., Nesnas, N., 2006. Oxidation of sulfonamide antimicrobials by ferrate(VI) $[Fe^{VI}O_4^{2-}]^+$. Environ. Sci. Technol. 40, 7222-7227.

Sharma, V.K., 2007. Disinfection performance of Fe(VI) in water and wastewater: a review. Water Sci. Technol. 55, 225-232.

Snyder, S.A., Keith, T.L., Verbrugge, D.A., Snyder, E.M., Gross, T.S., Kannan, K., Giesy, J.P., 1999. Analytical methods for detection of selected estrogenic compounds in aqueous mixtures.

Environ. Sci. Technol. 33, 2814-2820.

Sumpter, J.P., 1995. Feminized responses in fish to environmental estrogens. Toxicol. Lett. 82-83, 737-742.

Ternes, T.A., Stumpf, M., Mueller, J., Haberer, K., Wilken, R.D., Servos, M., 1999. Behavior and occurrence of estrogens in municipal sewage treatment plant-I. Investigation in Germany, Canada and Brazil. Sci. Total Environ. 225, 81-90.
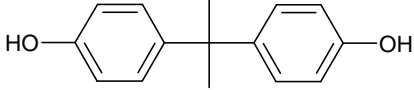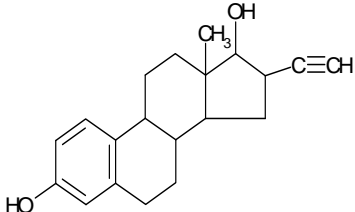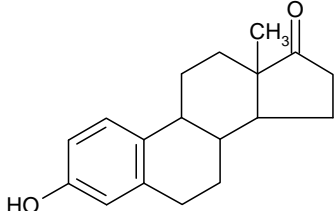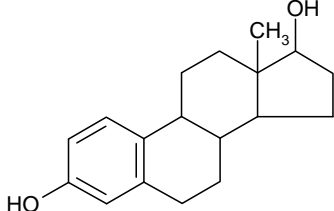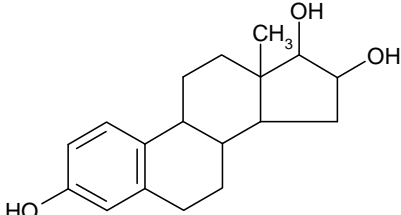
Toppari, J., Larsen, J.C., Christiansen, P., Giwercman, A., Grandjean, P., Guillette, L.J., Jegou, B., Jensen, T.K., Jouannet, P., Keiding, N., Leffers, H., McLachlan, J.A., Meyer, O., Muller, J., RajpertDeMeyts, E., Scheike, T., Sharpe, R., Sumpter, J., Skakkebaek, N.E., 1996. Male reproductive health and environmental xenoestrogens. Environ. Health. Persp. 104, 741-803.

Williams, C.L., Stancel, G.M., 1996. Estrogens and progestins, in:L.S. Goodman, A. Gilman (EDs.). The Pharmalcological Bases of Therapeutic, Macmilan, Indianapolis, In, 1411.

1   Table 1. Physicochemical Properties of the EDCs Studied

Chemical name	Structure	Molecular weight	pKa (25°C)	Log K_{ow}	Water solubility (mg L^{-1})
Bisphenol A (BPA)		228.29	9.6/10.2	3.32	120
17α-ethynylestr-adiol (EE2)		296.41	10.4	4.5×10^{-11}	4.2
Estrone (E1)		270.37	10.4	1.4×10^{-7}	3.4
β-estradiol (E2)		272.39	10.4	1.3×10^{-8}	3.9
estriol (E3)		288.39	10.4	6.7×10^{-15}	2.8

2

3

1   Table 2. Details of the HPLC Analytical Method for the Five EDCs

Chemical name	Retention time (min)	Mobile phase flow rate (mL min^{-1})	Detection wavelength (nm)
BPA	4.15	0.8	278
E1	5.57	0.8	280
E2	4.68	0.8	279
E3	3.35	0.8	280
EE2	4.83	0.8	280

2

3   Table 3. Details of the LC/MS-MS Analytical Method

Chemical name	Retention time (min)	[M-H]$^-$/ [M+H]$^+$	Gradient flow		
			Time (min)	DDW (%)	ACN (%)
BPA	27.98	227.3 ([M-H]$^-$)	0	100	0
			2	100	0
			6	70	30
			16	70	30
			30	30	70
			45	100	0

4   ACN means acetonitrile.

Table 4. Rate Constants of EDC Degradation with Ferrate(VI)

Compounds	k_1 (M^{-1} s^{-1})[a]	k_1' (M^{-1} s^{-1})[b]	k_2 (M^{-1} s^{-1})[c]	k_2' (M^{-1} s^{-1})[d]
BPA	2.80×10^2	5.16×10^2	8.20×10^2	7.76×10^4
EE2	3.05×10^2	8.52×10^2	9.10×10^2	5.11×10^5
E1	7.10×10^2	8.97×10^2	9.80×10^2	5.31×10^5
E2	7.32×10^2	9.41×10^2	1.08×10^3	5.40×10^5
E3	9.28×10^2	1.003×10^3	1.12×10^3	5.44×10^5
Rate constants given by Lee et al. 2005				
Compounds	k_{12} (M^{-1} s^{-1})	k_{21} (M^{-1} s^{-1})	k_{22} (M^{-1} s^{-1})	k_{23} (M^{-1} s^{-1})
EE2	-	$9.4(\pm0.2) \times 10^2$	$5.4(\pm0.2) \times 10^5$	-
E2	-	$1.0(\pm0.02) \times 10^3$	$5.4(\pm0.2) \times 10^5$	-
BPA	-	$8.2(\pm0.1) \times 10^2$	$8.0(\pm0.2) \times 10^4$	$2.6(\pm0.2) \times 10^5$

[a] FeO_4^{2-}; undissociated EDC
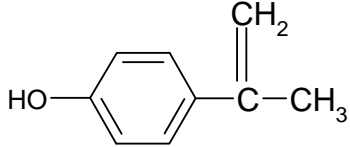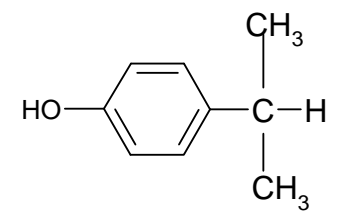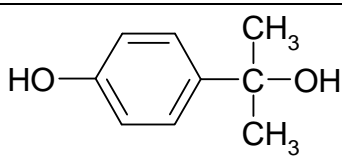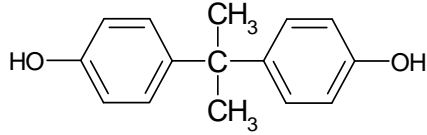
[b] FeO_4^{2-}; dissociated EDC

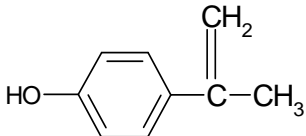[c] $HFeO_4^-$; undissociated EDC

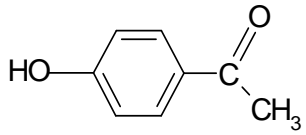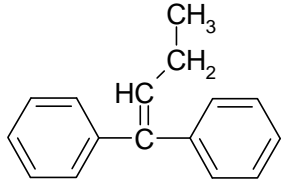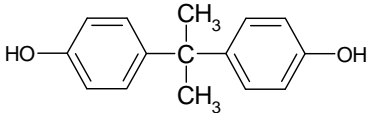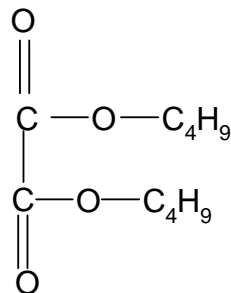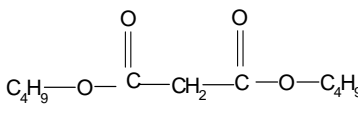[d] $HFeO_4^-$; dissociated EDC
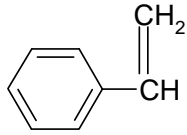
1   Table 5. Main Fragment Ions (m/z) and Abundance [%] of Reaction Intermediates Identified by

2   LC-ESI/MS-MS

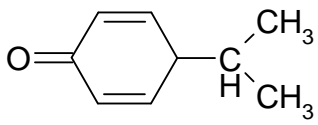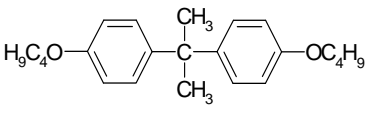| Peak No.	Retention time (min)	Detected ions (m/z) [% abundance]	Molecular weight (m/z)	Chemical names	Molecular structure
1	8.65	133 [100] 93 [25]	134	p-isopropenyl phenol	
2	9.60	135 [100] 93 [50] 120 [45]	136	p-isopropyl phenol	
3	13.05	161 [100] 114 [91] 144 [74]	152	4-isopropanol phenol	
4	29.30	227 [100] 212 [73] 133 [20]	228	Bisphenol A	

3

1　Table 6. Main Fragment Ions (m/z) and Abundance [%] of Reaction Intermediates Identified by

2　GC/MS-MS

Peak No.	Retention time (min)	Detected ions (m/z) [% abundance]	Molecular weight (m/z)	Chemical name	Molecular structure
1	4.49	104 [100] 77 [50] 51 [27]	104	Styrene	
2	10.54	134 [100] 119 [70] 91 [25]	134	p-isopropenyl phenol	
3	14.67	136 [29] 121 [100] 65 [40] 93 [40]	136	p-hydroxy acetophenone	
4	15.31	208 [79] 193 [66] 115 [100]	208	(1-phenyl-1-butenyl) benzene	
5	17.48	228 [28] 213 [100] 119 [50]	228	Bisphenol A	

3

1 Table 7. Main Fragment Ions (m/z) and Abundance [%] of Reaction Intermediates Identified by the

2 Butylesterification Derivative Method and GC/MS-MS

Peak No.	Retention time (min)	Detected ions (m/z) [% abundance]	Molecular weight (m/z)	Chemical name	Molecular structure
1	4.23	202 [10] 85 [100] 57 [15]	202	Oxalic acid	
2	5.27	105 [100] 57 [88] 56 [50]	216	Propanedioic acid	
3	6.57	91 [89] 77 [100] 136 [84] 108 [82]	136	4-isopropyl-cyl cohexa-2, 5-dienone	
4	17.91	325 [75] 340 [20] 73 [100]	340	BPA	

3

1 **List of figure captions**

2 Fig. 1: Comparison between experimental data and kinetic model for the degradation of EDCs by

3   ferrate

4

5 Fig. 2: Mass spectrum of BPA by LC/MS-MS

6

7 Fig. 3: BPA degradation and DOC reduction with reaction time at different ferrate:BPA molar

8   ratios (pH 9.2)

9

10 Fig. 4: The temporal formation and decay of the three identified intermediate products identified

11   by LC/MS-MS during the ferrate and BPA reaction

12

13 Fig. 5: The temporal formation and decay of the intermediate products identified by GC/MS-MS

14   during the ferrate and BPA reaction

15

16 Fig. 6: Proposed BPA degradation pathways by ferrate oxidation
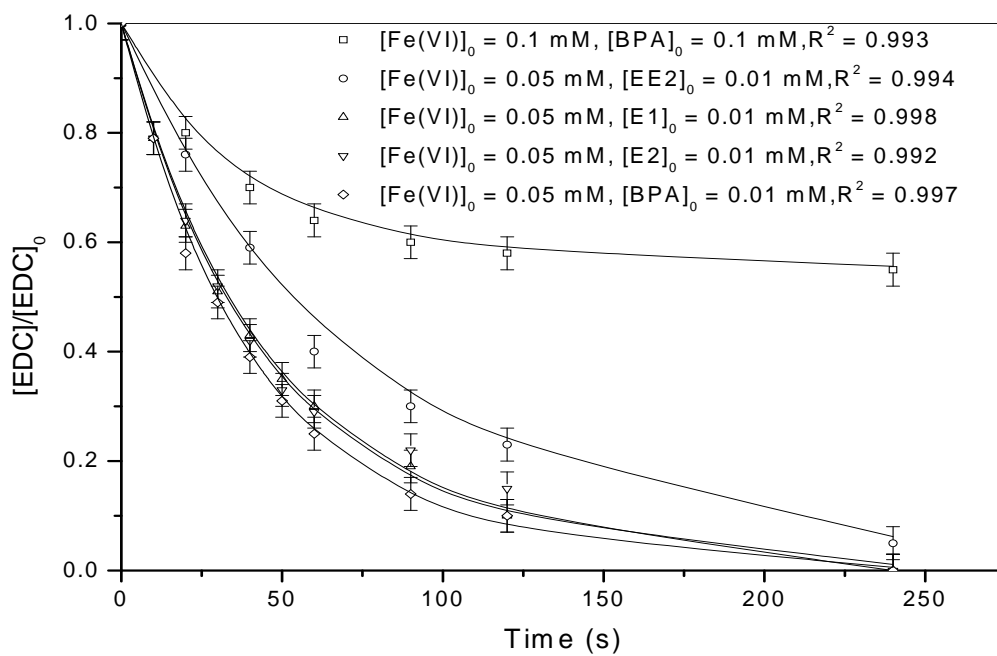
17

18

19

20

21

22

1   FIG. 1

2

3

The plot shows $[EDC]/[EDC]_0$ on the y-axis (from 0.0 to 1.0) versus Time (s) on the x-axis (from 0 to 250).

Legend:
- $[Fe(VI)]_0 = 0.1$ mM, $[BPA]_0 = 0.1$ mM, $R^2 = 0.993$
- $[Fe(VI)]_0 = 0.05$ mM, $[EE2]_0 = 0.01$ mM, $R^2 = 0.994$
- $[Fe(VI)]_0 = 0.05$ mM, $[E1]_0 = 0.01$ mM, $R^2 = 0.998$
- $[Fe(VI)]_0 = 0.05$ mM, $[E2]_0 = 0.01$ mM, $R^2 = 0.992$
- $[Fe(VI)]_0 = 0.05$ mM, $[BPA]_0 = 0.01$ mM, $R^2 = 0.997$

4

5

6

7

8

9

1 FIG. 2

2

3

4

5

Mass spectrum showing peaks at 227.3, 228.3, and 212.0 with molecular structures of bisphenol compounds. X-axis: m/z (from ~60 to 250), Y-axis: Intensity (0 to 6×10⁷).

6

7

8

9

10

11

12

13

14

15

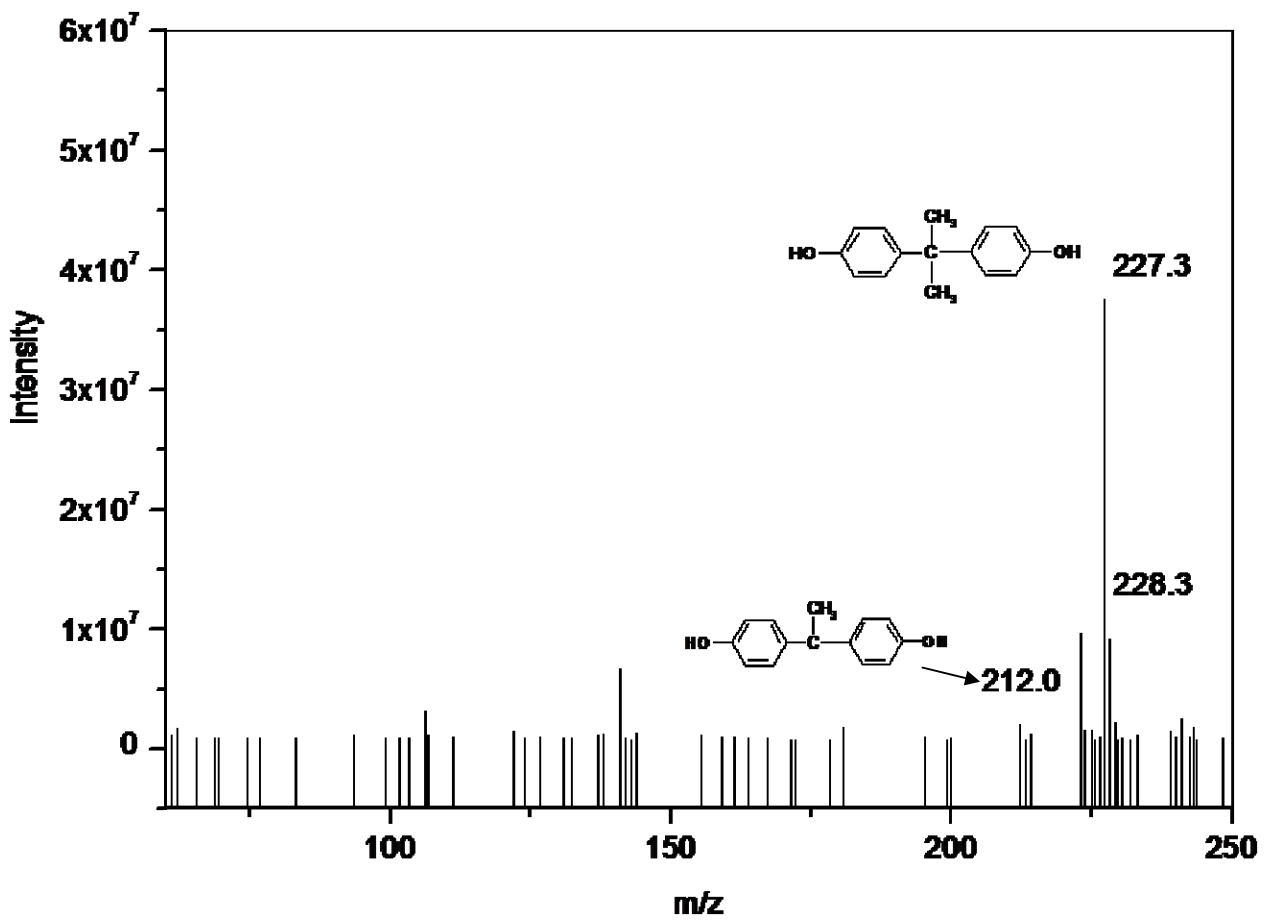16

17

18

19

20

21

22

23
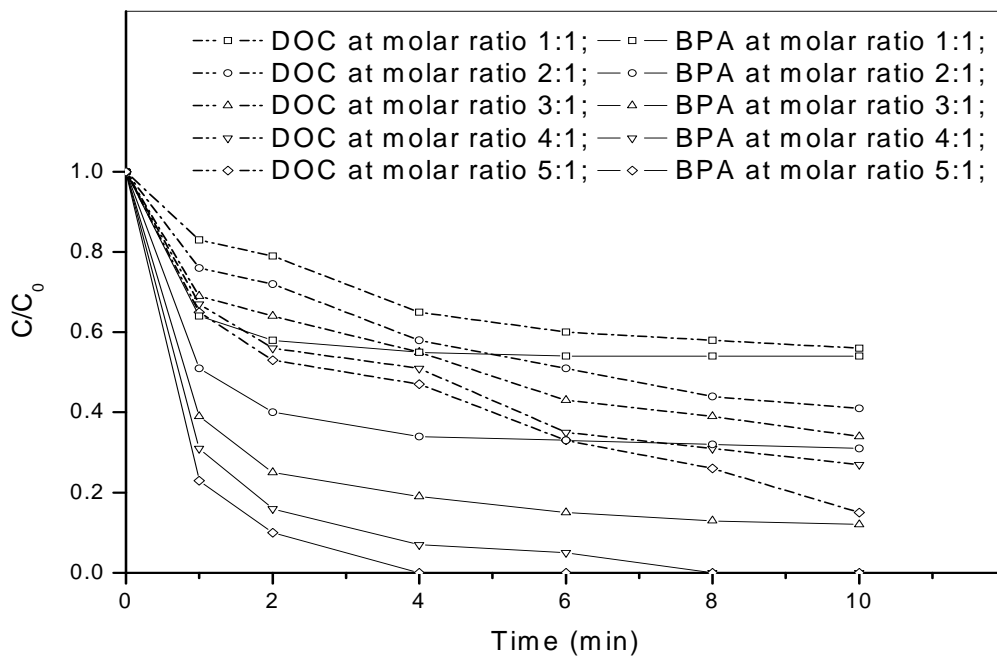
1   Fig. 3

2
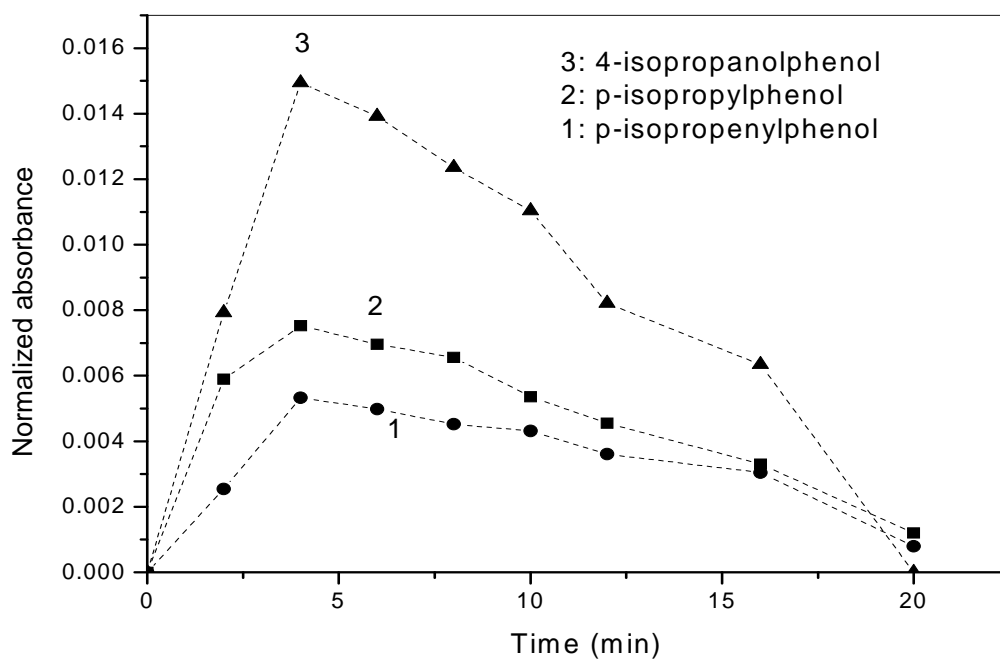
3

4

5

6

1   FIG. 4
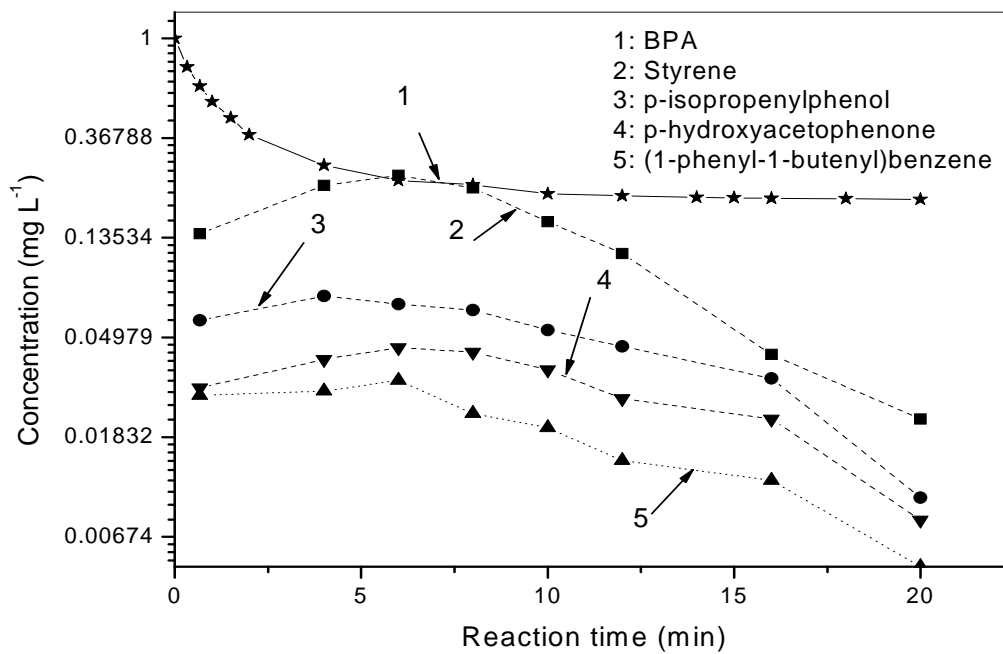
2

3

4

5

6

7

8

9

10

11

12

13

14

15

30

FIG. 5

FIG. 6